Chemistry & Biology, Vol. 11, 225–236, February, 2004, ©2004 Elsevier Science Ltd. All rights reserved. DOI 10.1016/j.chembiol.2004.01.014

Interaction of Epothilone Analogs with the Paclitaxel Binding Site: Relationship between Binding Affinity, Microtubule Stabilization, and Cytotoxicity

Rubén M. Buey,[1] J. Fernando Díaz,[1,*] José M. Andreu,[1] Aurora O'Brate,[2] Paraskevi Giannakakou,[2] K.C. Nicolaou,[3] Pradip K. Sasmal,[3] Andreas Ritzén,[3] and Kenji Namoto[3]

[1]Centro de Investigaciones Biológicas
Consejo Superior de Investigaciones Científicas
Ramiro de Maeztu 9
28040 Madrid
Spain

[2]Winship Cancer Institute
Emory University School of Medicine
Atlanta, Georgia 30322

[3]Department of Chemistry and
The Skaggs Institute for Chemical Biology
The Scripps Research Institute
10550 North Torrey Pines Road
La Jolla, California 92037
Department of Chemistry and Biochemistry
University of California, San Diego
9500 Gilman Drive
La Jolla, California 92093

Summary

The interactions of epothilone analogs with the paclitaxel binding site of microtubules were studied. The influence of chemical modifications in the C15 side chain and in C12 on binding affinity and microtubule elongation was characterized. Modifications favorable for binding affinity are (1) a thiomethyl group at C21 of the thiazole side chain, (2) a methyl group at C12 in *S* configuration, (3) a pyridine side chain with C15 in *S* configuration, and (4) a cyclopropyl moiety between C12 and C13. The same modification in different ligands has similar effect on affinity, allowing good structure-affinity characterization. The correlation between binding, microtubule stabilization, and cytotoxicity of the compounds has been determined, showing differential effects of the modifications. The binding constants correlate well with IC_{50} values, demonstrating that affinity measurements are a useful tool for drug design.

Introduction

The discovery in the early 1970s of paclitaxel in the bark of the pacific yew (*Taxus brevifolia*) [1] turned later into a revolution in the field of antimitotics. Paclitaxel and its derivatives, the best known of which is docetaxel (a semisynthetic analog obtained from the precursor baccatin III, which is obtained in large amounts from the leaves of the Mediterranean yew [*Taxus baccata*]), had at that time a unique mechanism of action among the other microtubule-perturbing drugs. While the classic microtubule-disrupting drugs (colchicine, vinblastine) block microtubule assembly by binding to the unassembled tubulin dimers and inactivating them, paclitaxel and docetaxel bind to microtubules, stabilizing them and blocking their dynamics [2, 3]. Nevertheless, despite their good activity against ovarian, metastatic breast, head and neck, and lung cancer [4], paclitaxel has two factors that hamper its applicability. First, its low aqueous solubility, and second, the development of pleiotropic drug resistance mediated both by the overexpression of the P-glycoprotein [5, 6] and the presence of mutations in β-tubulin [7, 8].

The discovery in recent years of several natural substances with a paclitaxel-like mechanism of action (epothilone, discodermolide, laulimalide, eleutherobin, peloruside, dictyostatin-1, taccalonolide, and jatrophane polyesters; [9–16]) opened new possibilities in the field. Of these compounds, the first one recognized as having a paclitaxel-like activity was an already known natural compound called epothilone [9], a secondary metabolite from the soil myxobacterium *Sorangium cellulosum* [17–19]. Epothilones are the most promising of this group of new paclitaxel-like compounds because they offer several advantages. First of all, while most of the other compounds are isolated from marine organisms in limited amounts, epothilone B can be obtained in kilogram amounts by fermentation [20]. Second, it has higher solubility in water than paclitaxel [19]. Third, it is a worse substrate for the P-glycoprotein than paclitaxel, and thus it is more effective than paclitaxel in cells showing multidrug resistance [9, 21, 22]. Finally, it has a simpler molecular architecture, which has allowed the total synthesis of the natural epothilones and many synthetic analogs [23–31].

The Nicolaou group initiated a program directed toward the design and synthesis of analogs [25–31], resulting in a large number of epothilone derivatives in which the essential positions C12 and C13 and the side chain in C15 have been modified in several ways (see structures of several of these compounds in Figure 1). But despite the effort made at characterizing the biological activity of the modifications, a limited effort has been made on the chemical characterization of the microtubule-epothilone interaction.

The study of the interaction between paclitaxel and its derivatives with the binding site shared with epothilones was greatly hampered by their mechanism of action [32–33]. Since they preferentially bind to the assembled form of tubulin inducing microtubule assembly, the assembly and binding are linked reactions [32]. Although empty sites can be assembled in the absence of ligand at high tubulin concentrations, the high affinity of the compounds makes it impossible to find conditions in which the reaction is not completely displaced toward the end state, making it difficult to obtain an exact measurement of the binding affinity of these compounds.

A procedure to stabilize assembled microtubules has made it possible to obtain taxoid binding sites that can be diluted to concentrations low enough to directly mea-

*Correspondence: fer@akilonia.cib.csic.es

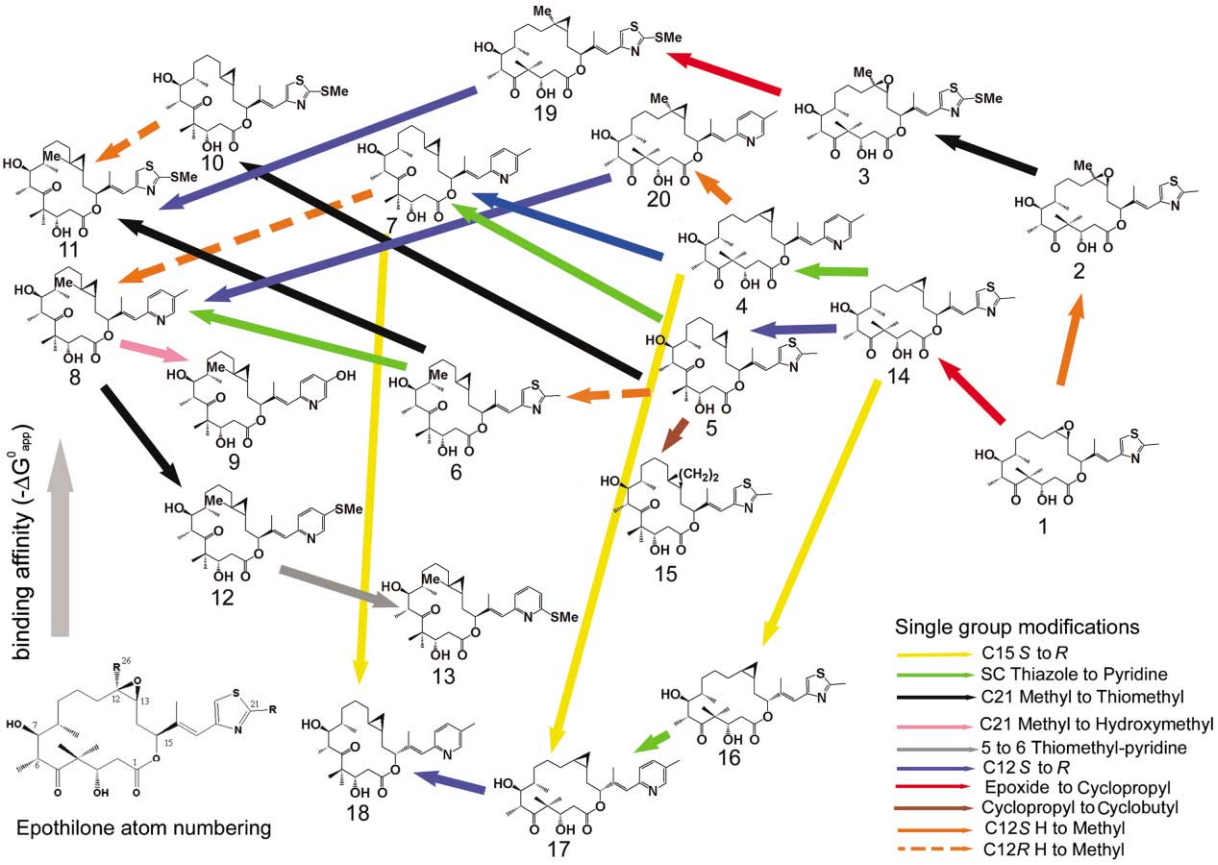

Figure 1. Scheme of the Structures of Epothilone Analogs Employed in This Study, the Chemical Differences between Them, and the Effect of These Modifications in the Free Energy of Binding to Their Site in Microtubules at 35°C

sure the binding affinity of two fluorescent derivatives of paclitaxel, Flutax-1 and Flutax-2 [34], and to develop a competition method that has been employed to measure the binding affinity of compounds that bind to the paclitaxel site, such as baccatin III [35], docetaxel and a 2-ethoxyestradiol analog (3,17β-diacetoxy-2ethoxy-6oxo-B-homo-estra-1,3,5(10)-triene) [36], epothilones A and B and several analogs [30], and paclitaxel [37], and also to distinguish them from compounds with similar effects, but which do not bind to the paclitaxel binding site, such as laulimalide [36].

The purposes of this study were as follows: (1) to determine the structure-affinity relationship of a group of chemically modified epothilones (Figure 1) and to learn how to increase epothilone binding affinity, and (2) to determine the correlations between affinity, cytotoxicity, and microtubule stabilization in order to facilitate the design of compounds with a higher activity in killing tumoral cells.

Results and Discussion

Mechanisms of Microtubule Stabilization by Epothilones

The biochemical mechanisms of epothilone-induced tubulin assembly were studied first in order to confirm that the compounds stabilize microtubules with a paclitaxel-like mechanism. The ability of two natural epothilones (epothilone A and epothilone B) to induce the assembly of GDP tubulin was tested. The inactive form of the protein (10 μM GDP tubulin in PEDTA 4 GDP buffer) undergoes ligand-induced assembly in the presence of stoichiometric amounts of the ligand as it does in the presence of paclitaxel. Electron microscopy controls were routinely performed on all assembled samples in order to confirm that the polymers were microtubules.

The stoichiometry of the binding was measured: 10 μM solutions of GDP or GTP tubulin in PEDTA 4 GDP for GDP tubulin or PEDTA 4 GTP buffer for GTP tubulin were incubated with increasing concentrations of epothilone A and epothilone B. The amount of ligand in the microtubule pellet was found to be 1 mol per mol of assembled tubulin, independently of the nucleotide bound (epothilone A, GDP tubulin 1.01 ± 0.05, GTP tubulin 0.99 ± 0.08; epothilone B, GDP tubulin 1.05 ± 0.07, GTP tubulin 1.02 ± 0.04). (All experimental notations in this manuscript are standard errors of the mean.) As for paclitaxel and docetaxel [32], in these conditions, assembly and binding of epothilone are linked; that is, every tubulin heterodimer assembled into microtubules has a molecule of epothilone bound (Figures 2A and 2B). Unless an excess of ligand is present in the assembly solution, all the ligand is bound to the assembled tubulin, and in the supernatant ligand is practically undetectable.

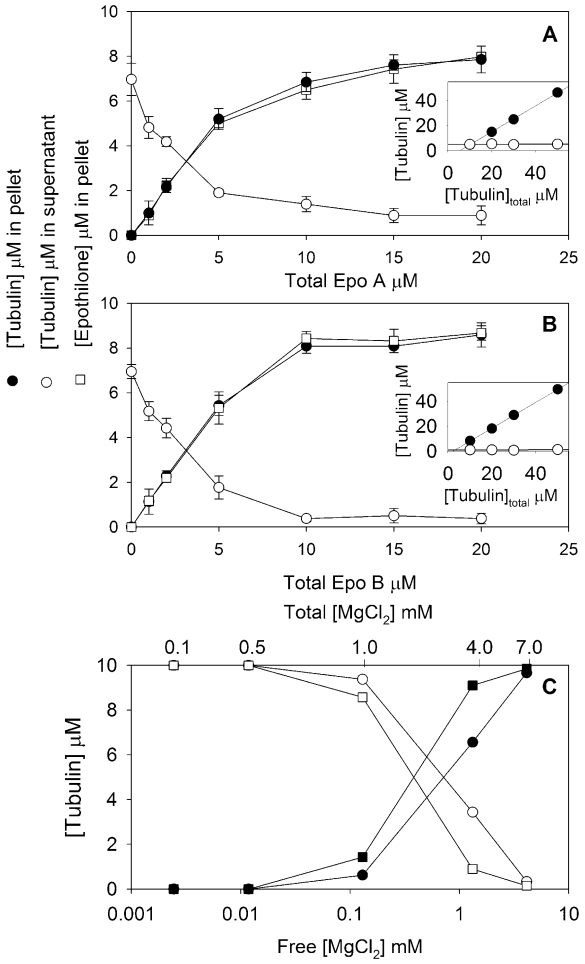

Figure 2. Biochemical Characterization of Epothilone-Induced Assembly of Tubulin

(A and B) Linkage between epothilone binding and tubulin assembly. GTP tubulin (10 μM) in PEDTA7 GTP was incubated with growing amounts of (A) epothilone A and (B) epothilone B. Tubulin concentrations in pellet (solid circles) and supernatants (empty circles) and epothilone concentrations in pellet (empty squares) were measured as described in Experimental Procedures. Insets: Critical concentrations of epothilone-induced GTP tubulin polymerization in PEDTA 4 GTP measured by centrifugation as described in Experimental Procedures. Tubulin concentrations in pellet, solid circles; in supernatants, empty circles.

(C) Requirement of Mg^{+2} for epothilone-induced tubulin assembly. GTP tubulin (10 μM) in PEDTA GTP buffer containing 12 μM epothilone A (circles) or epothilone B (squares) was incubated with growing amounts of $MgCl_2$. Tubulin concentrations in pellet (solid figures) and supernatants (empty figures) were measured by centrifugation. Note that the total [$MgCl_2$] mM upper scale is only for the reader's convenience and it is neither linear nor logarithmic.

Since the critical concentration (tubulin concentration in the supernatant) saturates with ligand concentration, the assembly process should follow the ligand-mediated pathway (see Supplemental Data available with this article online). A slight difference from the results obtained with paclitaxel [38] is that the tubulin concentration in the supernatant decreases at overstoichiometric concentrations of epothilone. Since at these epothilone concentrations (>1 μM free epothilone) all epothilone binding sites in the assembled microtubules are filled, this result might suggest binding of the ligand to unassembled tubulin (which will activate a second ligand-mediated pathway; see Equation S2A in the Supplemental Data).

The effect of Mg^{+2} on the epothilone-induced assembly was studied by adding growing concentrations of Mg^{+2} to 10 μM solutions of GTP tubulin containing 12 μM epothilone A or B in PEDTA GTP buffer. Epothilone-induced GTP tubulin assembly is dependent on Mg^{+2} (Figure 2C) as is the case for paclitaxel-induced GTP tubulin assembly [38]; both drugs require free concentrations of Mg^{+2} in the range of mM to induce assembly. Tubulin with GDP bound to the E site has the same Mg^{+2} requirement (data not shown).

The results above show that epothilones induce assembly in a paclitaxel-like way, assembly and binding being linked. This implies that in these experimental conditions the intrinsic binding cannot be isolated, which makes it extremely difficult to measure binding constants. Binding affinity of epothilones for microtubules seems to be high because free concentrations of ligand can only be detected at overstoichiometric ratios of ligand to tubulin. Experiments were run in which 5 μM empty ligand sites assembled from GTP tubulin in GAB 1 mM GTP were incubated with epothilone. Essentially all the ligand was found bound to the microtubules, indicating a binding affinity higher than micromolar. Since at least micromolar concentrations of tubulin are needed to assemble microtubules, in these experimental conditions the reaction is fully displaced toward the bound state and binding constants cannot be measured.

Binding of Epothilone Analogs to Stabilized Microtubules: Structure-Affinity Relationships and Increment Thermodynamic Parameters of Group Modification

Since it is not possible to measure the binding affinity of epothilone to ligand-free glycerol-induced microtubules, it was necessary to use microtubules stabilized against dilution and cold by gentle crosslinking [34, 35]. A test based in the displacement of a fluorescent taxoid probe (Flutax-2) from its binding site in these stabilized microtubules has been employed to measure binding affinities relative to that of Flutax-2 (Figure 3) [30, 35, 36]. The epothilone-microtubule binding was previously characterized using the natural compounds epothilones A and B. Epothilone B binds more strongly than epothilone A to its site in crosslinked microtubules (Ka 37°C in GAB 0.1 mM GTP; epothilone A, $2.93 \pm 0.44 \times 10^7$ M^{-1}; epothilone B, $60.8 \pm 10.1 \times 10^7$ M^{-1}); compatible values (epothilone A, $5 \pm 2 \times 10^7$ M^{-1}; epothilone B, $50 \pm 20 \times 10^7$ M^{-1}) were obtained using direct sedimentation measurements, which further validates the Flutax-2 displacement method. When compared with the paclitaxel group of drugs (Ka 37°C paclitaxel $1.07 \pm 0.11 \times 10^7$ M^{-1}, docetaxel $3.09 \pm 0.22 \times 10^7$ M^{-1} in GAB, 0.1 mM GTP), epothilone A binds with similar affinity to those ligands, while epothilone B is 20 times more powerful. The reaction is endothermic ($\Delta H_{EpoA} = -65 \pm 2$ kJ mol^{-1}, $\Delta H_{EpoB} = -70 \pm 7$ kJ mol^{-1}) and enthalpy driven.

The effect of Mg^{+2} ions, pH, and ionic strength in

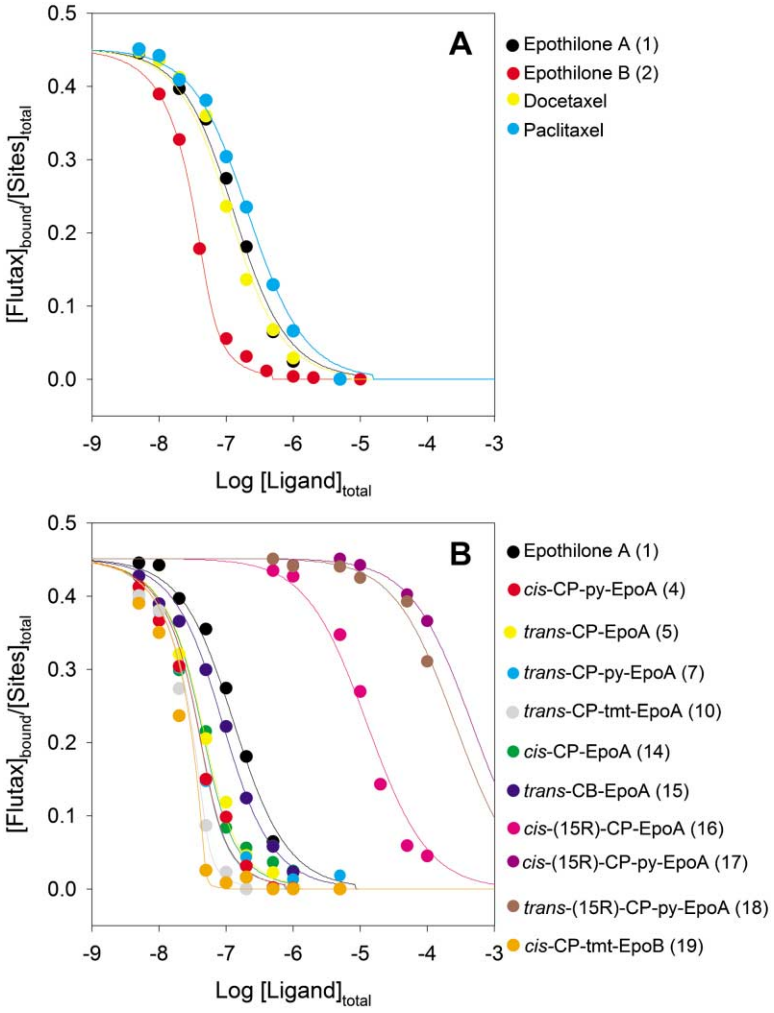

Figure 3. Competition between Flutax-2 and Epothilones for the Paclitaxel Binding Site

Displacement of the fluorescent taxoid Flutax-2 (50 nM) from microtubule binding sites (50 nM) by taxoids and epothilone analogs at 35°C. The points are data and the lines were generated with the best fit value of the binding equilibrium constant of each competitor, assuming a one to one binding to the same site. Ligands are as follows: in (A), epothilone A (compound **1**), black; epothilone B (compound **2**), red; docetaxel, yellow; paclitaxel, cyan. In (B), epothilone A, (compound **1**), black; *cis*-CP-py-EpoA (compound **4**), red; *trans*-CP-EpoA (compound **5**), yellow; *trans*-CP-py-EpoA (compound **7**), cyan; *trans*-CP-tmt-EpoA (compound **10**), gray; *cis*-CP-EpoA (compound **14**), green; *trans*-CB-EpoA (compound **15**), blue; *cis*-(15R)-CP-EpoA (compound **16**), pink; *cis*-(15*R*)-CP-py-EpoA (compound **17**), violet; *trans*-(15*R*)-CP-py-EpoA (compound **18**), brown; *cis*-CP-tmt-EpoB (compound **19**), orange. The lines shown with compounds **17** and **18** data correspond to simulated equilibrium binding constants of 6,000 and 12,000 M^{-1}, respectively (accurate determinations were precluded by the availability of more concentrated stock solutions).

the binding were characterized as well and have been shown to be weak in the range studied (1–9 mM Mg^{+2}, 0–1 M NaCl, 6–7 pH). Mg^{+2} ions, although necessary for ligand-induced assembly, have very little influence on the affinity of the drugs for their site, indicating that no additional Mg^{+2} ion is incorporated with ligand binding [39].

The structure-affinity relationship of the side chain and of the epoxy moiety of the epothilones has been studied using a selected group of chemically modified epothilones. Modifications have been made in positions 12, 15, and 21 of the epothilone molecules (Figure 1), which are important for activity [25]. These 20 compounds are related by a series of single group modifications, which are indicated by the colored arrows in Figure 1. The binding Gibbs free energy, enthalpy, and entropy changes can be estimated by measuring the binding affinities of the compounds to microtubules (Table 1 and Figure 3). The measurement of the affinities of a series of ligands for their site in a protein is a classical way to study the specificity of a protein-ligand interaction, and it can be a good approximation of the incremental binding energy provided by each group [40]. The incremental binding free energy change associated with the modification of ligand A into ligand B is defined as follows: $\Delta\Delta G^0_{app}(A \rightarrow B) = \Delta G^0_{app}(B) - \Delta G^0_{app}(A)$, and similarly for the incremental enthalpy and entropy changes. These incremental binding thermodynamic parameters are summarized in Table 2. Before starting the detailed analysis, we should keep in mind that although it is possible to dissect the incremental changes in Gibbs free energy into their enthalpy and entropy contributions, these individual contributions are difficult to analyze because of the enthalpy-entropy compensation effect (in aqueous solutions, enthalpy changes due to the presence of new electrostatic interactions can be transformed into entropy changes due to rearrangement of the water molecules [40, 41], which may lead to uncertainty in the interpretation of incremental enthalpy and entropy terms).

Modifications at C15 and the Side Chain

C15 Stereochemistry

The stereochemistry of this carbon is critical for epothilone binding affinity; C15 has to be in an *S* configuration in order to have a high-affinity binding. Molecular models built from the X-ray structure of epothilone A molecule [42] show that, with C15 in the *S* configuration, the side chain is roughly in the plane of the epothilone ring, while if the carbon is in the *R* configuration, the side chain is perpendicular to this plane. Epimerization of

Table 1. Apparent Thermodynamic Parameters of Binding of Epothilones to the Paclitaxel Binding Site of Microtubules, Determined from the Displacement of the Fluorescent Taxoid Flutax-2

Ligand	26°C	27°C	30°C	32°C	35°C	37°C	40°C	42°C	ΔG^0_{app}	ΔH^0_{app}	ΔS^0_{app}
	K (10^7 M^{-1})	K (10^7 M^{-1})	K (10^7 M^{-1})	K (10^7 M^{-1})	K (10^7 M^{-1})	K (10^7 M^{-1})	K (10^7 M^{-1})	K (10^7 M^{-1})	(kJ mol^{-1} at 35°C)	(kJ mol^{-1})	(J mol^{-1} K^{-1})
Paclitaxel	2.64 ± 0.17	2.19 ± 0.05	1.83 ± 0.09	1.81 ± 0.21	1.43 ± 0.17	1.07 ± 0.11	0.96 ± 0.14	0.94 ± 0.23	−42.2 ± 0.2	−51 ± 4	−28 ± 13
Docetaxel	6.95 ± 0.42	6.57 ± 0.52	5.42 ± 0.42	4.89 ± 0.38	3.93 ± 0.27	3.09 ± 0.22	2.89 ± 0.17	2.38 ± 0.11	−44.8 ± 0.2	−52 ± 2	−25 ± 8
Epothilone A [1]	7.48 ± 1.00	6.94 ± 1.08	5.81 ± 1.08	5.00 ± 0.49	3.63 ± 0.51	2.93 ± 0.44	2.32 ± 0.25	2.08 ± 0.21	−44.5 ± 0.3	−65 ± 2	−68 ± 9
Epothilone B [2]	150 ± 15	144 ± 32	120 ± 13	129 ± 30	75.0 ± 7.4	60.8 ± 10.1	49.4 ± 8.8	35.6 ± 2.6	−52.6 ± 0.5	−70 ± 7	−60 ± 23
tmt-EpoB [3]	414 ± 113	498 ± 202	258 ± 38	207 ± 26	250 ± 71	194 ± 33	234 ± 100	201 ± 112	−55.4 ± 0.6	−37 ± 11	62 ± 37
cis-CP-py-EpoA [4]	41.3 ± 8.3	40.7 ± 12.1	29.1 ± 7.8	31.1 ± 5.8	24.2 ± 4.8	19.4 ± 3.1	16.1 ± 3.2	13.5 ± 2.6	−49.4 ± 0.3	−54 ± 4	−16 ± 11
trans-CP-EpoA [5]	36.7 ± 1.5	35.1 ± 3.4	31.0 ± 1.9	27.3 ± 1.8	19.4 ± 1.0	15.3 ± 0.8	14.1 ± 0.8	12.1 ± 1.0	−48.6 ± 0.1	−58 ± 4	−28 ± 12
trans-CP-EpoB [6]	19.1 ± 3.5	20.7 ± 3.3	20.1 ± 2.5	18.8 ± 2.0	15.3 ± 1.5	11.4 ± 0.5	11.3 ± 0.7	10.7 ± 1.0	−48.2 ± 0.2	−35 ± 5	41 ± 18
trans-CP-py-EpoA [7]	96.6 ± 23.5	86.3 ± 12.2	90.6 ± 20.0	70.2 ± 6.2	48.3 ± 4.7	48.3 ± 8.8	40.5 ± 4.8	35.0 ± 3.5	−51.5 ± 0.2	−51 ± 5	7±15
trans-CP-py-EpoB [8]	32.4 ± 6.8	33.7 ± 5.3	34.0 ± 3.00	38.5 ± 4.8	34.5 ± 1.4	28.6 ± 2.5	23.5 ± 2.8	22.0 ± 2.2	−50.3 ± 0.1	−20 ± 7	95 ± 22
trans-CP-pyOH-EpoB [9]	29.5 ± 1.2	30.3 ± 1.3	28.3 ± 2.8	25.0 ± 2.6	20.0 ± 2.3	16.6 ± 2.3	15.6 ± 1.2	12.8 ± 0.6	−48.9 ± 0.3	−43 ± 4	19 ± 12
trans-CP-tmt-EpoA [10]	155 ± 27	191 ± 41	171 ± 42	173 ± 39	178 ± 48	141 ± 34	108 ± 29	121 ± 39	−54.5 ± 0.6	−21 ± 7	107 ± 23
trans-CP-tmt-EpoB [11]	59.5 ± 10.6	70.8 ± 8.0	73.3 ± 12.9	79.2 ± 10.3	62.6 ± 6.4	55.6 ± 6.4	60.2 ± 7.1	50.0 ± 4.0	−51.8 ± 0.3	−12 ± 7	127 ± 21
trans-CP-5tmpy-EpoB [12]	10.12 ± 1.34	17.1 ± 3.7	15.1 ± 2.8	14.0 ± 2.7	12.3 ± 2.2	10.4 ± 1.6	11.0 ± 1.9	7.9 ± 1.1	−47.7 ± 0.4	−36 ± 5	37 ± 16
trans-CP-6tmpy-EpoB [13]	3.30 ± 0.1	3.43 ± 0.29	3.19 ± 0.50	3.18 ± 0.32	2.46 ± 0.25	2.38 ± 0.4	2.15 ± 0.3	2.35 ± 0.46	−43.6 ± 0.3	−23 ± 4	67 ± 12
cis-CP-EpoA [14]	38.6 ± 3.3	36.4 ± 3.9	29.9 ± 3.4	30.4 ± 4.8	22.0 ± 3.3	17.5 ± 1.4	14.8 ± 1.2	12.0 ± 0.3	−49.2 ± 0.4	−57 ± 4	−26 ± 12
trans-CB-EpoA [15]	6.81 ± 0.19	6.67 ± 0.53	5.40 ± 0.48	5.08 ± 0.77	3.64 ± 0.41	3.12 ± 0.32	2.88 ± 0.37	2.70 ± 0.45	−44.5 ± 0.3	−49 ± 3	−15 ± 10
cis-(15R)-CP-EpoA(16)	0.0307 ± 0.005	0.0321 ± 0.005	0.0248 ± 0.0005	0.0250 ± 0.0025	0.0215 ± 0.0014	0.0187 ± 0.003	0.0172 ± 0.0014	0.0178 ± 0.0024	−31.4 ± 0.2	−31 ± 3	1 ± 10
cis-CP-tmt-EpoB [19]	3109 ± 1590	2189 ± 604	2053 ± 358	2670 ± 538	2055 ± 428	1565 ± 180	1049 ± 299	593 ± 113	−60.8 ± 0.5	ND	ND
cis-CP-py-EpoB [20]	131 ± 29	118 ± 48	98 ± 20	99 ± 23	71 ± 15	51 ± 6	53 ± 6	58 ± 16	−52.2 ± 0.4	−46 ± 7	20 ± 22

The values given in the table are averages and standard errors of each determination. The ΔG^0_{app} values of *cis*-(15*R*)-CP-py-EpoA(17) and *trans*-(15*R*)-CP-py-EpoA(18) were circa −22 and −24 kJ mol^{-1}, respectively, (35°C) from the data available.

Table 2. Incremental Thermodynamic Parameters of Binding of Epothilone Analogs to Microtubules

Single Group Modification	Compounds	$\Delta\Delta G^0_{app}$	$\Delta\Delta H^0_{app}$	$\Delta\Delta S^0_{app}$
		(kJ mol^{-1} at 308 °K)	(kJ mol^{-1})	(J mol^{-1}K^{-1})
C15 *S* to *R*	4→17	~27	ND	ND
	7→18	~27	ND	ND
	14→ 16	17.8 ± 0.3	26 ± 4	25 ± 11
C15 side chain thiazole→pyridine	5→7	−2.9 ± 0.2	7 ± 4	35 ± 14
	6→8	−2.1 ± 0.3	15 ± 9	54 ± 28
	14→4	−0.2 ±0.4	3 ± 4	10 ± 12
	16→17	~9.4	ND	ND
C21 methyl to thiomethyl	2→3	−2.8 ± 0.8	33 ± 13	122 ± 44
	5→10	−5.9 ± 0.6	37 ± 8	135 ± 24
	6→11	−3.6 ± 0.3	23 ± 9	86 ± 28
	8→12	2.6 ± 0.3	−16 ± 9	−58 ± 27
C21 methyl to hydroxymethyl	8→9	1.4 ± 0.3	−23 ± 8	−76 ± 25
5-thiomethyl-pyridine to 6-thiomethyl-pyridine	12→13	4.1 ± 0.5	13 ± 6	30 ± 20
C12 *S* to *R*	4→7	−2.1 ± 0.3	3 ± 5	23 ± 13
	14→5	0.6 ± 0.3	1 ± 4	−2 ± 12
	17→18	~−2	ND	ND
	19→11	9.0 ± 0.6	ND	ND
	20→8	1.9 ± 0.4	26 ± 10	75 ± 31
epoxide→cyclopropyl	1→14	−4.7 ± 0.4	8 ± 3	38 ± 11
	3→19	−5.4 ± 0.8	ND	ND
cyclopropyl→cyclobutyl	5→15	4.1 ± 0.2	8 ± 4	11 ± 11
C12*S* H to methyl	1→2	−8.1 ± 0.6	−5 ± 7	8 ± 25
	4→20	−1.8 ± 0.5	8 ± 8	36 ± 25
C12*R* H to methyl	5→6	0.4 ± 0.3	23 ± 6	69 ± 22
	7→8	1.2 ± 0.2	31 ± 9	88 ± 27
	10→11	2.7 ± 0.7	9 ± 10	20 ± 31

this chiral center from *S* to *R* results in low-affinity compounds, $\Delta\Delta G_{35°C}(4\rightarrow17) \approx +27$ kJ mol^{-1}, $\Delta\Delta G_{35°C}(7\rightarrow18) \approx +27$ kJ mol^{-1}, $\Delta\Delta G_{35°C}(14\rightarrow16) = +17.8$ kJ mol^{-1} (each transformation is named with the numbers of the original and the resulting compound; see Figure 1), suggesting that the side chain in the new position is not able to bind the site, with the subsequent loss of binding enthalpy ($\Delta\Delta H^0_{app}(14\rightarrow16) = 26$ kJ mol^{-1}). Moreover, the new position of the side chain in the C15*R* compounds may interfere with the binding of the rest of the molecule. The reason for this might be purely steric, since the larger the side chain, the larger the loss in binding affinity (compound **16** with a thiazole group retains larger affinity than compounds **17** and **18** with pyridine side chains).

It has to be pointed out that a similar effect is observed if the stereochemistry of C13 is changed from *S* to *R* as in C13*R*-cyclopropyl-epothilones, which have been obtained as an unexpected result in the synthetic process of *cis*-CP-EpoA (compound **14**) [25, 28]. Those ligands are inactive, probably because this modification will place the C15 side chain in a similar position (under the plane of the ring) to that occupied by the side chain in the C15*R* compounds **16**, **17**, and **18**.

Change of the C15 Side Chain Ring

Two different groups have been employed as C15 side chain ring, thiazole and pyridine. Out of the four examples studied, the modification was favorable in two cases, neutral in one, and unfavorable in one case, depending on the stereochemistry of C12 and C15. With C12 and C15 in their natural *S* configuration, the modification was practically neutral, $\Delta\Delta G_{35°C}(14\rightarrow4) = -0.2$ kJ mol^{-1}. The modification thiazole for pyridine was favorable with C12 in the *R* configuration: $\Delta\Delta G_{35°C}(5\rightarrow7) = -2.9$ kJ mol^{-1}, $\Delta\Delta G_{35°C}(6\rightarrow8) = -2.1$ kJ mol^{-1}. The increase in binding affinity is due to the entropic term, since the contribution of the enthalpy term is unfavorable. As discussed above, when C15 is of the *R* configuration, the introduction of the larger side chain results in a loss of affinity, $\Delta\Delta G_{35°C}(16\rightarrow17) \approx +9.4$ kJ mol^{-1}.

Change of the C21 Substituent

Three different groups (methyl, hydroxymethyl, and thiomethyl) have been employed as substituents of the side chain ring at position C21. The effect of the substituents in the binding to the paclitaxel site depends on the side chain ring to which they are attached.

When the side chain ring is a thiazole, the change made was methyl to thiomethyl. The change is favorable in the three examples, independently from C12 configurations: $\Delta\Delta G_{35°C}(2\rightarrow3) = -2.8$ kJ mol^{-1}, $\Delta\Delta G_{35°C}(5\rightarrow10) = -5.9$ kJmol^{-1}, $\Delta\Delta G_{35°C}(6\rightarrow11) = -3.6$ kJ mol^{-1}. In the three cases, the thermodynamic analysis of the modification shows that the modification is highly unfavorable in the enthalpy term, but it is more strongly favorable in the entropy term, turning the binding reaction from enthalpy driven into entropy driven.

Compounds having a thiomethyl-thiazole side chain include the most powerful epothilone analogs studied, *cis*-CP-tmt-EpoB ($\Delta G_{35°C}$ (**19**) = −60.8 kJ mol^{-1}), tmt-EpoB ($\Delta G_{35°C}$ (**3**) = −55.4 kJ mol^{-1}), and *trans*-CP-tmt-EpoA ($\Delta G_{35°C}$ (**10**) = −54.5 kJ mol^{-1}). The second one is just the result of this single modification in the natural epothilone EpoB. In the case of compound **19**, the binding affinity of the compound (~10^{10} M^{-1}) is very much higher than those of the fluorescent probe (~10^7 M^{-1}), precluding reliable dissection of the incremental changes in Gibbs free energy into their enthalpy and entropy contributions.

When the side chain is pyridine (with C12 being of the

R configuration), the same modification (thiomethyl for methyl) results in a loss of binding affinity: $\Delta\Delta G_{35°C}(8\rightarrow12) = +2.6$ kJ mol. A possible explanation is that the change from thiazole to pyridine may have placed the methyl group in a better position for interaction, and the introduction of the sulfur spacer between the ring and the methyl, which has a favorable effect in the case of the thiazole side chain (it may place the methyl in a similar position to the change from thiazole to pyridine), has a unfavorable effect in this case because it may displace the methyl group from its ideal position. The change from methyl for hydroxymethyl in the pyridine group has a slightly unfavorable effect: $\Delta\Delta G_{35°C}(8\rightarrow9) = +1.4$ kJ mol^{-1}. Both modifications are favorable from the enthalpic point of view but unfavorable in the entropic term. The change of the position of the thiomethyl group from position C5 to position C6 of the pyridine ring is unfavorable, $\Delta\Delta G_{35°C}(12\rightarrow13) = +4.1$ kJ mol^{-1}; in this case, an increment in enthalpy, $\Delta\Delta H_{app}(12\rightarrow13) = 13$ kJ mol^{-1}, is not compensated with the increment in entropy, $\Delta\Delta S_{app}(12\rightarrow13) = 30$ kJ mol^{-1}K^{-1}.

C12 Modifications

C12 Stereochemistry

The result of the change of the stereochemistry of C12 from *S* to *R* depends on the side chain bound to the C15 and on the substituents at C12. For epothilone A analogs, (1) if the side chain is thiazole, the observed change in affinity is almost neutral, $\Delta\Delta G_{35°C}(14\rightarrow5) = +0.6$ kJ mol^{-1}; (2) if the side chain is pyridine, the change has a favorable effect, $\Delta\Delta G_{35°C}(4\rightarrow7) = -2.1$ kJ mol^{-1}. This modification has no large effects on the enthalpy and entropy of binding. The same transformation applied to a low-affinity ligand *cis*-(15*R*)-CP-py-EpoA results in a similar change in binding affinity $\Delta\Delta G_{35°C}(17\rightarrow18) \approx -2$ kJ mol^{-1}. For epothilone B analogs, the modification is unfavorable with side chain thiazole, $\Delta\Delta G_{35°C}(19\rightarrow11) = +9.0$ kJ mol^{-1}, and side chain pyridine, $\Delta\Delta G_{35°C}(20\rightarrow8) = +1.9$ kJ mol^{-1}. In this case, the enthalpic contribution is so highly unfavorable that the favorable entropic contribution is not enough to compensate for it.

Chemical Modifications of the Epoxy Group

Another modification examined is the transformation of the epoxy group of epothilone A into a cycloalkyl group. A cyclopropyl group increases the binding affinity: $\Delta\Delta G_{35°C}(1\rightarrow14) = -4.7$ kJ mol^{-1}, $\Delta\Delta G_{35°C}(3\rightarrow19) = -5.4$ kJ mol^{-1}.

A further modification was the increase in size of the cycloalkyl group by substituting the cyclopropyl group by a cyclobutyl, $\Delta\Delta G_{35°C}(5\rightarrow15) = +4.1$ kJ mol^{-1}. The decrease of binding affinity is due to an increase in the enthalpy of binding, which is not compensated by the entropic benefit of the more hydrophobic group.

Introduction of a Methyl Group in C12

This modification occurs in the natural epothilone B, and it strongly favors binding in the natural epothilone with C12 in *S* configuration ($\Delta\Delta G_{35°C}(1\rightarrow2) = -8.1$ kJ mol^{-1}) with moderate benefits in both enthalpic and entropic terms of the free energy change. The modification is also favorable (although not so strongly) in the other example studied ($\Delta\Delta G_{35°C}(4\rightarrow20) = -1.8$ kJ mol^{-1}). The rest of the examples available in this study have this carbon in the *R* configuration, and in all these cases the modification results in a loss of binding affinity: $\Delta\Delta G_{35°C}(5\rightarrow6) = +0.4$ kJ mol^{-1}, $\Delta\Delta G_{35°C}(7\rightarrow8) = +1.2$ kJ mol^{-1}, $\Delta\Delta G_{35°C}(10\rightarrow11) = +2.7$ kJ mol^{-1}. The effect of these modifications on the thermodynamic parameters of binding is an increase in the enthalpy of binding, which is not compensated by the entropic benefit; the net result being unfavorable for affinity.

Overview of Epothilone Structure-Activity Relationships

Apart from the natural modification, the methyl group in C12*S* which renders EpoB from EpoA, the most successful modifications for affinity are the introduction of the thiomethyl group in C21 as thiazole substituent and the exchange of the epoxide moiety for a cyclopropyl. Surprisingly, the result of the introduction of the thiomethyl group is a complete change of the thermodynamic parameters of the binding, turning an enthalpy-driven reaction (the binding of compounds **1**, **2**, **5**, **14**, **15**, and **16**, i.e., the compounds with a methyl-thiazole side chain except compound **6** proceed with a unfavorable entropy contribution to the free energy of binding) into an entropy-driven reaction (the binding of compounds **3**, **10**, and **11**, i.e., all compounds with a thiomethyl-thiazole side chain proceed with a large favorable entropic contribution to the free energy of binding). Changes in the hydrophobic surface of the ligand at selected points may possibly improve binding by enhancing certain hydrophobic interactions. In fact, the paclitaxel binding site has been described as a hydrophobic pocket [43]. Another example of this is the substitution of thiazole for pyridine (which is favorable or neutral as long as C15 is in *S* configuration [compounds **4**, **7**, **8**]). The increase in binding affinity results from a similar effect to that produced by the introduction of the thiomethyl group as thiazole substituent; that is, an increase of the entropic contribution to the free energy of binding, which compensates for a moderate decrease in the enthalpic component. It is tempting to suggest in explanation of these results that the increase in size of the group to which the methyl group is attached places the methyl substituent in a better position for a hydrophobic interaction, leading to an entropy-driven reaction. Any further modification of the methyl substituent of the pyridine ring results in loss of affinity due to a large decrease of the entropy of binding.

The change of the stereochemistry of C12 from *S* to *R* has as well a weakly favorable entropic effect, so it may as well involve a modification of a hydrophobic interaction. The effect of the introduction of a methyl group at position C12 has opposite effects, depending on the stereochemistry. In the C12*S* configuration (the natural one), it has a favorable effect: $\Delta\Delta G_{35°C}(1\rightarrow2) = -8.1$ kJ mol^{-1}, $\Delta\Delta G_{35°C}(4\rightarrow20) = -1.8$ kJ mol^{-1}. If C12 is in the *R* configuration, the effect is favorable in the entropic term and unfavorable in the enthalpy term; in this case, the gain in the entropic term can not compensate the loss, resulting in a decrease of binding affinity. This is also observed in the case of the favorable modification $\Delta\Delta G_{35°C}(4\rightarrow20) = -1.8$ kJ mol^{-1}, with C12 in the *S* configuration and a cyclopropyl instead of epoxide, which is far less favorable than $\Delta\Delta G_{35°C}(1\rightarrow2) = -8.1$ kJ mol^{-1}, favorable for both terms of the free energy. This

Table 3. Comparison of Ligand Binding Affinities at 37°C, the Critical Concentration Values of Ligand-Induced Microtubule Assembly, and the Cytotoxicity of Epothilones and Paclitaxel against 1A9 Human Ovarian Carcinoma Cells

Compound	Cr μM	Kel_2 *1e5 (M^{-1})	$1/K_{bin1}$ (nM)	IC50 (nM)[a]
Paclitaxel	4.24 ± 0.49	2.35 ± 0.24	93 ± 9[b]	1.30 ± 0.22
Docetaxel	1.52 ± 0.25	6.58 ± 0.93	32 ± 3	0.45 ± 0.25
Epothilone A [1]	5.11 ± 0.15	2.93 ± 0.44	34 ± 4	3.10 ± 0.72
Epothilone B [2]	1.17 ± 0.12	8.55 ± 0.80	1.6 ± 0.1	0.30 ± 0.05
tmt-EpoB [3]	0.72 ± 0.089	13.89 ± 1.53	0.51 ± 0.07[b]	0.17 ± 0.08
cis-CP-py-EpoA [4]	1.53 ± 0.10	6.53 ± 0.40	5.2 ± 0.8	1.40 ± 0.45
trans-CP-EpoA [5]	1.27 ± 0.21	7.87 ± 1.11	6.5 ± 0.1	2.70 ± 0.10
trans-CP-EpoB [6]	2.19 ± 0.30	4.57 ± 0.55	8.8 ± 0.4[b]	15.00 ± 0.00
trans-CP-py-EpoA(7)	1.53 ± 0.10	6.53 ± 0.40	2.1 ± 0.4	0.62 ± 0.17
trans-CP-py-EpoB(8)	1.19 ± 0.21	8.40 ± 1.26	3.5 ± 0.3[b]	1.70 ± 0.76
trans-CP-pyOH-EpoB(9)	1.70 ± 0.18	5.88 ± 1.26	6.0 ± 0.6	1.70 ± 1.12
trans-CP-tmt-EpoA(10)	1.44 ± 0.12	6.94 ± 0.53	0.71 ± 0.14[b]	1.20 ± 0.67
trans-CP-tmt-EpoB(11)	1.36 ± 0.21	7.35 ± 0.98	1.8 ± 0.2	3.50 ± 1.64
trans-CP-5tmpy-EpoB(12)	2.54 ± 0.10	3.94 ± 0.15	9.6 ± 1.3[b]	14.20 ± 5.73
trans-CP-6tmpy-EpoB(13)	9.65 ± 2.46	1.04 ± 0.21	42 ± 7[b]	114.00 ± 0.00
cis-CP-EpoA(14)	0.93 ± 0.17	10.75 ± 1.66	5.7 ± 0.4	1.60 ± 0.12
trans-CB-EpoA(15)	2.97 ± 0.12	3.36 ± 0.13	32 ± 3	25.5 ± 1.5
cis-(15*R*)-CP-EpoA(16)	>50	<0.2	~5300	225
cis-(15*R*)-CP-py-EpoA(17)	>50	<0.2	~170,000	>300 (inactive)
trans-(15*R*)-CP-py-EpoA [18]	>50	<0.2	~83,000	>300 (inactive)
cis-CP-tmt-EpoB [19]	0.38 ± 0.07	26.3 ± 4.1	0.063 ± 0.006	0.1 ± 0.0
cis-CP-py-EpoB [20]	0.71 ± 0.03	14.1 ± 0.6	1.9 ± 0.1	0.3 ± 0.1

[a] Data taken from [29–31].

[b] These data differ from those previously published [30] since they have been measured again with higher precision.

suggests that the effect should be due to the loss of the negative charge provided by the oxygen, whose interactions with the tubulin may be favored by the presence of the methyl at C12.

The effect of the modifications is accumulative, resulting in the EpoB analog with the C12-C13 *cis* cyclopropyl moiety, and the thiomethyl-thiazole as side chain (*cis*-CP-tmt-EpoB) having the largest affinity of all the compounds studied, $\Delta G_{35°C}$(*cis*-CP-tmt-EpoB) = −60.8 ± 0.5 kJ mol^{-1}.

Comparison between Epothilone Binding Affinities and Their Microtubule Stabilization Activity

In order to better understand the structure/activity relationship of this group of epothilone analogs, it should be taken into account that the effect of the ligands on the system is microtubule stabilization. Thus, it would be interesting to quantitatively compare microtubule assembly induced by these ligands. If, as discussed above, the epothilone-induced assembly mechanism follows the ligand-mediated pathway, the apparent critical concentration (Cr) of ligand-induced assembly measured in the presence of an excess of ligand is in a good approximation of the critical concentration of the microtubules bound to epothilone (see Supplemental Data available with this article online) (i.e., $1/Cr = K_{app} = K_{el2}$). K_{el2} can be then directly compared to the binding constants of the ligand to their empty site in microtubules, K_{bin1}.

The critical concentrations of microtubule assembly induced by paclitaxel, docetaxel, and the epothilone analogs at 37°C were measured (Table 3). Out of the compounds studied, the strongest assembly inductor is compound **19**, the one with the highest affinity, Cr 0.31 ± 0.07 μM, while the weakest inductor is compound **13**, Cr 10.75 ± 1.66 μM, which is the epothilone with the lowest affinity (except for the inactive compounds **16**, **17**, and **18**). Epothilone B is a more powerful assembly inducer than epothilone A. The critical concentration of epothilone B-induced assembly is four times lower (Cr EpoB, 1.17 ± 0.12 μM; Cr EpoA, 5.11 ± 0.15 μM).

The comparison between the binding affinities of the ligands to their site K_{bin1} and the equilibrium constant for the growth reaction K_{el2} (Figure 4A) shows that they correlate ($r^2 = 0.62$), although the changes in the apparent free energy of elongation are much smaller than those in the apparent free energy of binding (slope = 0.39). The analogs that stabilize microtubules better than corresponds to their binding activity (i.e., those significantly over the best regression line) are compounds **5** and **14** (the two *cis-trans* isomers of CP-EpoA) and compounds **8** and **20** (the two *cis-trans* isomers of CP-py-EpoB). On the other hand, compounds **10** and **13**, both containing the thiomethyl substituent, are significantly under the best regression line, being the ones with the worst K_{el}/K_{bin} ratio. It should be noted that there are also two trends in the data that may point to the influence of the substitutions in the microtubule stabilization activity of the ligands. (1) In addition to compounds **5** and **14**, epothilone A and two other epothilone A analogs (compounds **4** and **15**) are slightly over the best regression line, which is only the case for epothilone B analogs containing pyridine in the side chain (compounds **8**, **9, and 20**). (2) Compounds that contain the thiomethyl substituent tend to have lower assembly induction power than expected, i.e., compounds **10**, **11**, **12**, **13**, and **19**.

Although assembly induction and binding affinity are not necessarily related, since they are different reactions with different intrinsic equilibrium binding constants,

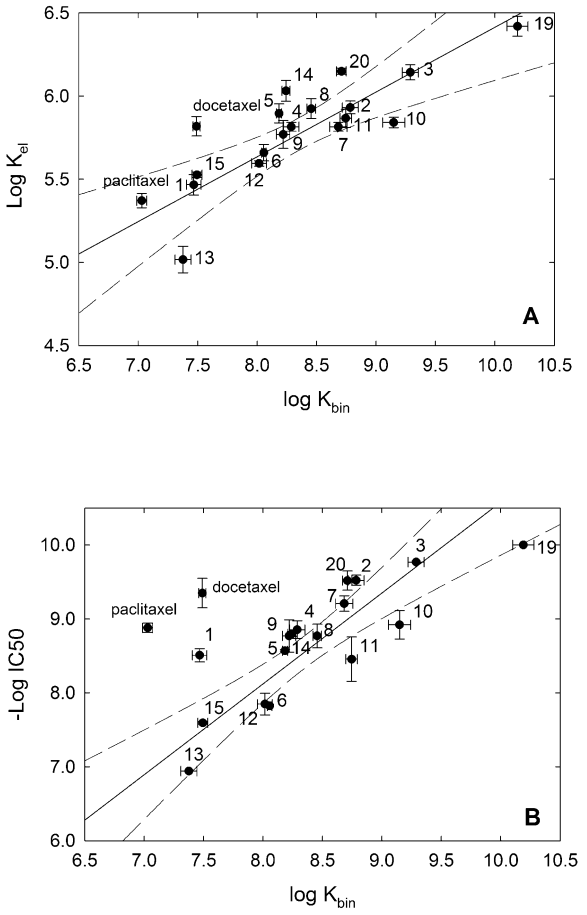

Figure 4. Comparison of Binding Affinity, Microtubule Stabilization, and Cytotoxicity of the Epothilone Analogs

(A) Dependence of the elongation constant of ligand-induced assembly K_{el2} on the binding constant to the paclitaxel site of microtubules K_{bin1}. The data of paclitaxel and docetaxel are not employed for the regression.

(B) Dependence of the IC_{50} of ligands against 1A9 human ovarian carcinoma cells on the binding constant to paclitaxel binding site of microtubules K_{bin1}. The data of paclitaxel, docetaxel, and epothilone A are not employed for the regression. Solid lines are the best linear regressions to the experimental data; dashed lines are the 95% confidence intervals of the regressions.

K_{bin1} and K_{el2} (see Supplemental Data), the experimental results indicate that they are somehow linked. However, it should be noted that the chemical features that are more effective in increasing binding affinity are not necessarily the same ones that improve the assembly induction capacity.

Correlation between Binding Affinities and Cytotoxicity

Figure 4B shows the IC_{50} of the compounds in 1A9 cells (a human ovarian carcinoma cell line). The plot of log IC_{50} versus log K_{bin1} shows that both values correlate well (r^2 0.76, slope 1.22), suggesting that binding affinity is an important parameter involved in cytotoxicity. Cytotoxicity and affinity data are listed in Table 3.

Apart from epothilone A, which is clearly over the best regression line, having a much better cytotoxicity than expected from its binding affinity, two groups of compounds whose separate best regression lines differ by at least 2σ intervals (data not shown) may be distinguished. The first one (compounds **2**, **3**, **4**, **5**, **7**, **8**, **9**, **14**, **15**, and **20**) has a higher cytotoxicity/affinity ratio than the second group of six compounds (compounds **6**, **10**, **11**, **12**, **13**, and **19**), which include five of the six compounds containing the thiomethyl group. The first group of compounds have an IC_{50} which is 2 to 3 times lower than their dissociation constants from stabilized microtubules (a difference that might be related to a similar difference between the binding affinities of stabilized microtubules and MAPs (microtubule associated proteins) containing microtubules for the fluorescent probe ligand employed [34, 37]. The second group of compounds have IC_{50}s that are half of their Kd, so this group of compounds is around 5 times less effective (relative to their binding affinity) in killing tumor cells than the other group. It should be noted that all the compounds of this group have a highly favorable entropic contribution to the binding affinity.

The two natural compounds, epothilone A and epothilone B, which are the ones with the lowest enthalpy of binding ($\Delta H_{app} = -65 \pm 2$ and -70 ± 7 kJ mol^{-1}, respectively), are the ligands with the highest ratio between IC_{50} and binding constant ($IC_{50}/K_{bin1} = 11$ and 5.3, respectively). This suggests that modifications that improve the favorable enthalpic component of binding would render analogs with increased cytotoxicity.

In summary, it can be said that the measurement of binding affinities is a useful tool for designing compounds with a larger cytotoxicity, since (1) favorable and unfavorable contributions to the binding of the different groups are accumulative, so new epothilone analogs with higher affinity can be designed on the basis of the results. (2) It is possible to dissect the effect of the modifications on the entropic and enthalpy terms of the free energy of binding. Modifications that increase binding but have a unfavorable contribution on the enthalpic term seem to be less effective in increasing cytotoxicity. (3) With the assay employed, it is possible to rapidly rank the effect in the binding affinity of single modifications on epothilones.

Although there is a correlation between K_{el2} and IC_{50} ($r = 0.68$) (Table 3), this is a trivial consequence of the correlation between K_{bin} and K_{el} previously discussed. There are several reasons to choose binding affinities as a better design tool than microtubule stabilization. First, at the IC_{50} concentrations, the free concentration of ligand in the cells should be of the order of nanomolar (not to be confused with the total concentration of ligand in the cells, which is much higher [44] since the ligands accumulate in the cells due to binding to the cellular microtubules). These concentrations are too low to induce microtubule stabilization in vitro. With the known binding and elongation equilibrium constants of the assembly process, it can be shown that the apparent microtubule critical concentration should not be affected at such low ligand-free concentrations (see Figure S1 in the Supplemental Data). It implies that the effect of the ligand at IC_{50} concentrations should not be noticed in microtubule stabilization but in the microtubule dynamics. Second, binding affinities are within the same

order of magnitude of the IC_{50} of the ligand, and changes in binding affinity are reflected in relatively similar changes in IC_{50}, whereas critical concentrations are three orders of magnitude higher than IC_{50}, and large differences in cytotoxicity are only reflected in small changes of the critical concentration (Table 3). And third, from the practical point of view the determination of critical concentrations requires biochemical manipulations of a labile protein, while determination of the binding constants of several ligands can be made in a 96-well plate using stabilized binding site preparations.

Significance

Epothilones A and B induce microtubule assembly in a paclitaxel-like way with a mechanism thermodynamically equivalent to a ligand-mediated protein association.

The influence of chemical modifications in the C15 side chain and at C12 of epothilone on binding affinity and microtubule stabilization were characterized, showing that the incremental binding free energy changes of single modifications provide a good estimation of the binding energy provided by each group. Modifications increasing binding affinity are as follows: (1) a thiomethyl group at C21 of the thiazole side chain, (2) a methyl group at C12 in the *S* configuration, (3) a pyridine side chain with C15 in the *S* configuration, and (4) a cyclopropyl moiety between C12 and C13. Modifications 1 and 3 are unfavorable in the enthalpy term of the free energy and are very favorable in the entropy term, suggesting that they place the methyl substituent in a better position for a hydrophobic interaction. The ligand having all these favorable modifications, *cis*-CP-tmt-EpoB, has the highest affinity (Ka 2.1 $\pm$ 0.4 $\times$ 10^{10} M^{-1} at 35°C).

This study has provided useful information about the influence of single group modifications on three activities: binding affinity, microtubule stabilization, and cytotoxicity. There are differential effects of the modifications, as follows: (1) epothilone A analogs are more effective microtubule stabilizers than epothilone B analogs, (2) a thiomethyl group at position C21 of the thiazole side chain is more effective in increasing binding affinity than in increasing microtubule stabilization, and (3) compounds with a favorable entropic contribution to binding are less effective in killing tumoral cells than those with a favorable enthalpic contribution. Nevertheless, the influence of the modifications on the three activities correlate well, so it can be concluded that the determination of binding affinity of epothilone analogs is a useful parameter to be maximized in order to have compounds with higher activity.

Experimental Procedures

Purified calf brain tubulin and chemicals were as described [32]. Epothilones A and B and the epothilone analogs were synthesized as described [28, 31] and were employed as 10 mM stock solutions in DMSO, which were stored at −20°C. The solubility of these compounds in water was greater than 50 μM. The concentrations of epothilone A and epothilone B were determined spectrophotometrically in ethanol employing the following extinction coefficients: epothilone A, ϵ_{249} 12500 M^{-1} cm^{-1}; epothilone B, ϵ_{249}, 14100 M^{-1} cm^{-1} [19]). Paclitaxel (Taxol) was provided by the late M. Suffness from the National Cancer Institute (Bethesda, MD). Docetaxel (Taxotere) was kindly provided by Rhône Poulenc Rorer, Aventis (Schiltigheim, France). Flutax-2 (7-*O*-[*N*–(4′-2,7-Difluoro-Fluoresceincarbonil)-L-alanyl]-paclitaxel) was provided by Prof. Francisco Amat-Guerri; it was dissolved in DMSO and its concentration was measured spectrophotometrically (ϵ_{496} = 49100 cm^{-1} M^{-1} in 50 mM sodium phosphate, 0.5% SDS, pH 7.0 [34]).

Buffers employed were as follows: GAB, glycerol assembly buffer, 3.4 M glycerol, 10 mM sodium phosphate, 1 mM EGTA, 6 mM MgCl2 (pH 6.5); PEDTA GDP, 10 mM sodium phosphate, 1mM EDTA, 1 mM GDP, (pH 6.7); PEDTA GTP, PEDTA GDP plus 1 mM GTP; PEDTA 4 GDP, PEDTA GDP with 4 mM MgCl2; PEDTA 4 GTP, PEDTA GTP with 4 mM MgCl2; PEDTA 7 GDP, PEDTA GDP with 7 mM MgCl2; PEDTA 7 GTP, PEDTA GTP with 7 mM MgCl2.

Preparation of Stabilized Microtubules

Stabilized crosslinked microtubules were prepared as described [37]. To determine the exact concentration of sites in the microtubules, 5 μM Flutax-2 was added to a solution containing 2 μM total tubulin concentration (as determined spectrophotometrically) in GAB, 0.1 mM GTP, in the presence or absence of 100 μM docetaxel. The samples were centrifuged at 50,000 rpm for 20 min in a TL100 rotor employing a Beckman Optima TLX ultracentrifuge. Supernatants were taken and an aliquot of them was diluted 1:5 in 10 mM phosphate, 1% SDS buffer (pH 7.0). The pellets were resuspended in the same buffer and diluted 1:5. The concentrations of Flutax-2 in pellets and supernatants were measured fluorometrically using λ_{exc} 495, λ_{ems} 520 in Shimadzu RF-540 fluorimeter, employing spectrophotometrically calibrated Flutax-2 standards. The amount of Flutax-2 pelleted in the presence of 100 μM docetaxel had to be substracted from the amount of Flutax-2 pelleted in absence of docetaxel. The resulting amount is the concentration of reversibly bound Flutax-2 in saturation conditions, i.e., the concentration of paclitaxel binding sites in the sample, which can be extrapolated to the stock. Between 95% and 100% of the assembled tubulin dimers were found to bind taxoid.

Equilibrium Binding Constants of the Ligands to Microtubules

The equilibrium binding constants of the different ligands to the paclitaxel binding site of assembled microtubules were measured by the displacement of a fluorescent taxoid probe (Flutax-2) from its binding site. The displacement isotherm of each ligand was measured at least four times in two different plates with a fluorescence polarization microplate reader, as described [35]. Crosslinked stabilized microtubules that had been stored under liquid nitrogen were employed.

A mixture of 50 nM paclitaxel binding sites and 50 nM Flutax-2 in the desired buffer was sampled in a 96-well plate. Increasing concentrations of the competitor ligands were added to the wells. After mixing the samples for 10 min by shaking at 250 rpm, their anisotropies were measured after 20 min incubation at the desired temperatures using a POLARSTAR BMG plate reader in the polarization mode, employing the 480-P excitation filter and the 520-P emission filters. A sample containing 50 nM paclitaxel binding sites was employed as blank, and a 50 nM solution of Flutax-2 in GAB, 0.1 mM GTP was employed as anisotropy standard (polarization p = 0.07). Measurements of the anisotropy of Flutax-2 completely displaced (in the presence of a large excess of docetaxel) and, in absence of the competitor ligand, are required for data processing.

The binding constants of the reference ligand Flutax-2 were measured by centrifugation and fluorescence anisotropy at each temperature and buffer condition (Table 2; [34] and this work).

The binding of Flutax-2 (reference ligand) in the presence of the competitor ligand (ν_x = $|Flutax\text{-}2|_{bound}/|Sites|$) is calculated from the fluorescence anisotropy measurements as follows. Since the anisotropy is an additive property, the anisotropy of a given mixture is the sum of the anisotropy of its components. The anisotropies of Flutax-2 in the two reference states (the nondisplaced r_o and the fully displaced r_{min}) are known, and the binding of the reference ligand Flutax-2 in the absence of competitor (ν_o) is calculated from

the concentration of Flutax-2 binding sites and the binding constant of Flutax-2, so the measured anisotropy values r_x are transformed into fractional saturation values ν_x employing Equation 1:

$$vx = \frac{vo^* (rx - r\,\mathrm{min})}{(ro - r\,\mathrm{min})}. \quad (1)$$

The fractional saturation values of Flutax-2 at different competitor concentrations were best fitted to the equilibrium binding constant of the competitor assuming unitary stoichiometry and the binding constant of the reference ligand (Flutax-2) with a PC program (J.F.D., unpublished program Equigra v5).

Once the equilibrium binding constants are measured at different temperatures, the standard free energy of binding at a given temperature is calculated from the binding constant as $\Delta G_{0app} = -RTLnK_a$, the standard enthalpy of the binding reaction is calculated from the representation of LnK_a versus 1/T (Van't Hoff representation), and the slope of this representation multiplied by $-R$ is equal to $-\Delta H_{0app}$. The standard entropy of binding is calculated from the representation of ΔG_{0app} versus T; the slope of this representation is equal to ΔS_{0app}.

The equilibrium binding constants of epothilones A and B to its site in microtubules were also measured by centrifugation. Sixty-five milliliters of 10 nM sites in crosslinked microtubules were incubated for 30 min at 25°C with increasing concentrations of the ligand. The mixtures were then centrifuged for 55 min at 45,000 rpm in a Ti45 rotor in a XL-90 Ultracentrifuge. The supernatants were removed and the pellets were resuspended in 20 ml of 10 mM sodium phosphate at 4°C and incubated for 1 hr. The supernatants were extracted with 2 × 50 ml dichloromethane, and the pellets were extracted with 2 × 20 ml of the same solvent. This procedure has been found to quantitatively separate the ligands, which enter the organic phase, from the tubulin, which precipitates at the water-organic interface. After vacuum evaporation of the dichloromethane, the residues were each dissolved in 30 μl 70% methanol in water (v/v). Standard solutions of epothilones A and B were processed analogously. HPLC analysis of the samples was performed in a C-18 column (Supercosil, LC18-DB, 250 × 4.6 mm, 5 μm bead size) developed isocratically with 70% methanol in water (v/v) at a flow rate of 1 ml/min. Ligand concentrations in pellet and supernatants were determined by integration of eluted peaks and comparison to the areas produced by known quantities of the compound.

Ligand-Induced Microtubule Assembly

GTP or GDP tubulin samples in the desired buffer were prepared as described [38]. Prior to assembly, the ligand was added at 0°–2°C and the solutions were warmed to 37°C. The time needed to reach equilibrium depends on the tubulin concentration and the ligand employed. The polymers were sedimented at 90,000 × g for 20 min in a TLA 100 rotor preequilibrated at 37°C. The supernatants were separated by aspiration. If the ligand content of the pellets was extracted, they were resuspended in cold 10 mM phosphate (pH 7.0) buffer, otherwise 1% SDS was added to the buffer. Tubulin concentrations in supernatants and pellets were measured fluorometrically employing tubulin as standard.

The ligand content of supernatants and pellets was extracted three times with one volume of dichloromethane, the solvent was evaporated, and the residues were dissolved in 100 μl of 70% MeOH −30% H_2O. Standards of paclitaxel and epothilones were extracted in order to quantify the samples. The standards and samples were analyzed by HPLC as above.

The critical concentrations of ligand-induced tubulin assembly were measured in PEDTA 4 GTP. GTP tubulin at several concentrations ranging between 1 and 50 μM was incubated at 37°C for 45 min in the presence of the ligand at a concentration 10% in excess over the tubulin. The polymers were sedimented at 90,000 × g for 20 min in a TLA 100 rotor preequilibrated at 37°C. The supernatants were separated by aspiration, pellets were resuspended in 10 mM phosphate, 1% SDS (pH 7.0). Tubulin concentrations in supernatants and pellets were measured fluorometrically employing tubulin as standard. The critical concentration of tubulin is the concentration of tubulin in the supernatant (which is equal to the tubulin concentration given by the extrapolation to zero of the plot concentration of tubulin in the pellets versus total concentration) [45, 46]. Apparent polymer growth equilibrium constants were estimated as the reciprocal critical concentrations for polymerization (see Supplemental Data) [45, 46]. The assembled polymers were observed by electron microscopy as described [38].

Supplemental Data

Model mechanisms of ligand-induced assembly are discussed in the supplemental data available at http://www.chembiol.com/cgi/content/full/11/2/225/DC1.

Acknowledgments

We wish to thank Prof. Francisco Amat-Guerri for Flutax-2, Matadero Madrid Norte S.A., and José Luis Gancedo S.L. for providing the calf brains for tubulin purification. This work was supported in part by grants BIO2001-1725 from MCyT to J.F.D., 07B/0026/2002 from Comunidad de Madrid to J.M.A., and the Avon Foundation with funds raised through the Avon Breast Cancer Crusade and NIH Prostate Cancer SPORE Grant CA-58236 to P.G. R.M.B. was supported by a MECD FPU predoctoral fellowship. K.C.N. acknowledges the Skaggs Institute for Chemical Biology, the National Institutes of Health, and Novartis for their financial support.

Received: September 29, 2003
Revised: November 21, 2003
Accepted: November 21, 2003
Published: February 20, 2004

References

1. Wani, M.C., Taylor, H.L., Wall, M.E., Coggon, P., and McPhail, A.T. (1971). Plant antitumor agents. VI. The isolation and structure of taxol, a novel antileukemic and antitumor agent from *Taxus brevifolia*. J. Am. Chem. Soc. *93*, 2325–2327.
2. Schiff, P.B., Fant, J., and Horwitz, S.B. (1979). Promotion of microtubule assembly in vitro by taxol. Nature *277*, 665–667.
3. Schiff, P.B., and Horwitz, S.B. (1980). Taxol stabilizes microtubules in mouse fibroblast cells. Proc. Natl. Acad. Sci. USA *77*, 1561–1565.
4. Choy, H. (2001). Taxanes in combined modality therapy for solid tumors. Crit. Rev. Oncol. Hematol. *37*, 237–247.
5. Gottesman, M.M., Pastan, I., and Ambudkar, S.V. (1996). P-glycoprotein and multidrug resistance. Curr. Opin. Genet. Dev. *6*, 610–617.
6. Litman, T., Druley, T.E., Stein, W.D., and Bates, S.E. (2001). From MDR to MXR: new understanding of multidrug resistance systems, their properties and clinical significance. Cell. Mol. Life Sci. *58*, 931–959.
7. Giannakakou, P., Sackett, D.L., Kang, Y.K., Zhan, Z., Buters, J.T., Fojo, T., and Poruchynsky, M.S. (1997). Paclitaxel-resistant human ovarian cancer cells have mutant beta-tubulins that exhibit impaired paclitaxel-driven polymerization. J. Biol. Chem. *272*, 17118–17125.
8. Gonzalez-Garay, M.L., Chang, L., Blade, K., Menick, D.R., and Cabral, F. (1999). A beta-tubulin leucine cluster involved in microtubule assembly and paclitaxel resistance. J. Biol. Chem. *274*, 23875–23882.
9. Bollag, D.M., McQueney, P.A., Zhu, J., Hensens, O., Koupal, L., Liesch, J., Goetz, M., Lazarides, E., and Woods, C.M. (1995). Epothilones, a new class of microtubule-stabilizing agents with a taxol-like mechanism of action. Cancer Res. *55*, 2325–2333.
10. Ter Haar, E., Kowalski, R.J., Hamel, E., Lin, C.M., Longley, R.E., Gunasekera, S.P., Rosenkranz, H.S., and Day, B.W. (1996). Discodermolide, a cytotoxic marine agent that stabilizes microtubules more potently than Taxol. Biochemistry *35*, 243–250.
11. Long, B.H., Carboni, J.M., Wasserman, A.J., Cornell, L.A., Casazza, A.M., Jensen, P.R., Lindel, T., Fenical, W., and Fairchild, C.R. (1998). Eleutherobin, a novel cytotoxic agent that induces tubulin polymerization, is similar to paclitaxel (Taxol). Cancer Res. *58*, 1111–1115.
12. Mooberry, S.L., Tien, G., Hernández, A.H., Plubrukarn, A., and Davidson, B.S. (1999). Laulimalide and isolaulimalide, new pacli-

taxel-like microtubule-stabilizing agents. Cancer Res. *59*, 653–660.

13. Hood, K.A., West, L.M., Rouwé, B., Northcote, P.T., Berridge, M.V., Wakefield, S.J., and Miller, J.H. (2002). Peloruside A, a novel antimitotic agent with paclitaxel like microtubule-stabilizing activity. Cancer Res. *62*, 3356–3360.
14. Isbrucker, R.A., Cummings, J., Pomponi, S.A., Longley, R.E., and Wright, A.E. (2003). Tubulin polymerizing activity of dictyostain-1, a polyketide of marine sponge origin. Biochem. Pharmacol. *66*, 75–82.
15. Tinley, T.L., Randall-Hlubek, D.A., Leal, R.M., Jackson, E.M., Cessac, J.W., Quada, J.C., Jr., Hemscheid, T.K., and Mooberry, S.L. (2003). Taccalonolides E and A: plant-derived steroids with microtubule stabilizing activity. Cancer Res. *63*, 3211–3220.
16. Miglietta, A., Gabriel, L., Appendino, G., and Bocca, C. (2003). Biological properties of jatrophane polyesters new microtubule interacting agents. Cancer Chemother. Pharmacol. *51*, 67–74.
17. Höfle, G., Bedorf, N., Steinmetz, H., Schomburg, D., Gerth, K., and Reichenbach, H. (May, 1993). Epothilone, deren Herstellungsverfahren so wie sie enthaltende Mittel. German patent DE 4138042 A1.
18. Gerth, K., Bedorf, N., Höfle, G., Irschik, H., and Reichenbach, H. (1996). Epothilones A and B: antifungal and cytotoxic compounds from *Sorangium cellulosum* (myxobacteria). J. Antibiot. (Tokyo) *49*, 560–563.
19. Höfle, G., Bedorf, N., Steinmetz, H., Schomburg, D., Gerth, K., and Reichenbach, H. (1996). Epothilone A and B novel 16-membered macrolides with cytotoxic activity: isolation, crystal structure and conformation in solution. Angew. Chem. Int. Ed. Engl. *35*, 1567–1569.
20. Mulzer, J. (2000). Epothilone B and its derivatives as novel antitumour drugs: total and partial synthesis and biological evaluation. Monatsh. Chem. *131*, 205–238.
21. Kowalski, R.J., Giannakakou, P., and Hamel, E. (1997). Activities of the microtubule-stabilizing agents epothilones A and B with purified tubulin and in cells resistant to paclitaxel (Taxol®). J. Biol. Chem. *272*, 2534–2541.
22. He, L., Orr, G.A., and Horwitz, S.B. (2001). Novel molecules that interact with microtubules and have functional activity similar to Taxol. Drug Discov. Today *6*, 1153–1164.
23. Balog, A., Meng, D., Kamenecka, T., Bertinato, P., Su, D.S., Sorensen, E.J., and Danishefsky, S.J. (1996). Total synthesis of (-)-Epothilone A. Angew. Chem. *35*, 2801–2803.
24. Nicolaou, K.C., Winssinger, N., Pastor, J., Ninkovic, S., Sarabia, F., He, Y., Vourloumis, D., Yang, Z., Li, T., Giannakakou, P., et al. (1997). Synthesis of epothilones A and B in solid and solution phase. Nature *387*, 268–272.
25. Nicolaou, K.C., Ray, M., Finlay, V., Ninkovic, S., King, N.P., He, Y., Li, T., Sarabia, F., and Vourloumis, D. (1998). Synthesis and biological properties of C12,13-cyclopropyl-epothilone A and related epothilones. Chem. Biol. *5*, 365–372.
26. Nicolaou, K.C., Scarpelli, R., Bollbuck, B., Werschkun, B., Pereira, M.M., Wartmann, M., Altmann, K.H., Zaharevitz, D., Gussio, R., and Giannakakou, P. (2000). Chemical synthesis and biological properties of pyridine epothilones. Chem. Biol. *7*, 593–599.
27. Nicolaou, K.C., Hepworth, D., King, N.P., Finlay, M.R., Scarpelli, R., Pereira, M.M., Bollbuck, B., Bigot, A., Werschkun, B., and Winssinger, N. (2000). Total synthesis of 16-desmethylepothilone B, epothilone B10, epothilone F, and related side chain modified epothilone B analogues. Chemistry *6*, 2783–2800.
28. Nicolaou, K.C., Namoto, K., Li, J., Ritzén, A., Ulven, T., Shoji, M., Zaharevitz, D., Gussio, R., Sackett, D.L., Ward, R.D., et al. (2001). Synthesis and biological evaluation of 12,13-cyclopropyl and 12,13-cyclobutyl epothilones. Chembiochem *1*, 69–75.
29. Nicolaou, K.C., Namoto, K., Ritzén, A., Ulven, T., Shoji, M., Li, J., D'Amico, G., Liotta, D., French, C.T., Wartman, M., et al. (2001). Chemical synthesis and biological evaluation of cis- and trans-12,13-cyclopropyl and 12,13-cyclobutyl epothilones and related pyridine side chain analogues. J. Am. Chem. Soc. *123*, 9313–9323.
30. Nicolaou, K.C., Ritzén, A., Namoto, K., Buey, R.M., Díaz, J.F., Andreu, J.M., Wartmann, M., Altmann, K.H., O'Brate, A., and Giannakakou, P. (2002). Chemical synthesis and biological evaluation of novel epothilone B and trans-12,13-cyclopropyl epothilone B analogues. Tetrahedron *58*, 6413–6432.
31. Nicolaou, K.C., Sasmal, P.K., Rassias, G., Reddy, M.V., Altmann, K.H., Wartmann, M., O'Brate, A., and Giannakakou, P. (2003). Design, synthesis, and biological properties of highly potent Epothilone B analogs. Angew. Chem. Int. Ed. Engl. *42*, 3515–3520.
32. Díaz, J.F., Menéndez, M., and Andreu, J.M. (1993). Thermodynamic of ligand-induced assembly of tubulin. Biochemistry *32*, 10067–10077.
33. Evangelio, J.A., Abal, M., Barasoain, I., Souto, A.A., Lillo, M.P., Acuña, A.U., Amat-Guerri, F., and Andreu, J.M. (1998). Fluorescent taxoids as probes of the microtubule cytoskeleton. Cell Motil. Cytoskeleton *39*, 73–90.
34. Díaz, J.F., Strobe, R., Engelborghs, Y., Souto, A.A., and Andreu, J.M. (2000). Molecular recognition of taxol by microtubules. Kinetics and thermodynamics of binding of fluorescent taxol derivatives to an exposed site. J. Biol. Chem. *275*, 26265–26276.
35. Andreu, J.M., and Barasoain, I. (2001). The interaction of baccatin III with the taxol binding site of microtubules determined by a homogeneous assay with fluorescent taxoid. Biochemistry *40*, 11975–11984.
36. Pryor, D.E., O'Brate, A., Bilcer, G., Díaz, J.F., Wang, Y., Wang, Y., Kabaki, M., Jung, M.K., Andreu, J.M., Ghosh, A.K., et al. (2002). The microtubule stabilizing agent laulimalide does not bind in the taxoid site, kills cells resistant to paclitaxel and epothilones, and may not require its epoxide moiety for activity. Biochemistry *41*, 9109–9115.
37. Díaz, J.F., Barasoain, I., and Andreu, J.M. (2003). Fast kinetics of taxol binding to microtubules. Effects of solution variables and microtubule-associated proteins. J. Biol. Chem. *278*, 8407–8419.
38. Diaz, J.F., and Andreu, J.M. (1993). Assembly of purified GDP-tubulin into microtubules induced by taxol and taxotere: reversibility, ligand stoichiometry, and competition. Biochemistry *32*, 2747–2755.
39. Wyman, J., and Gill, S.J. (1990). Binding and Linkage (Mill Valley, CA: University Science Books).
40. Fersht, A. (1999). Forces between molecules, and binding energies. In Structure and Mechanism in Protein Science (New York: Freeman and Company), pp. 324–348.
41. Dunitz, J.D. (1995). Win some, lose some: enthalpy-entropy compensation in weak intermolecular interactions. Chem. Biol. *2*, 709–712.
42. Höfle, G., Glaser, N., Kiffe, M., Hecht, J., Sasse, F., and Reichenbach, H. (1999). N-Oxidation of epothilone A-C and O-Acil rearrangement to C-19- and C-21-substituted epothilones. Angew. Chem. Int. Ed. Engl. *38*, 1971–1974.
43. Lowe, J., Li, H., Downing, K.H., and Nogales, E. (2001). Refined structure of alpha beta-tubulin at 3.5 A resolution. J. Mol. Biol. *313*, 1045–1057.
44. Yvon, A.M., Wadsworth, P., and Jordan, M.A. (1999). Taxol suppresses dynamics of individual microtubules in living human tumor cells. Mol. Biol. Cell *10*, 947–959.
45. Oosawa, F., and Asakura, S. (1975). Thermodynamics of the Polymerization of Protein (London: Academic Press).
46. Andreu, J.M., and Timasheff, S.N. (1986). The measurement of cooperative protein self-assembly by turbidity and other techniques. Methods Enzymol. *130*, 47–59.

Supplemental Data

Interaction of Epothilone Analogs with the Paclitaxel Binding Site: Relationship between Binding Affinity, Microtubule Stabilization, and Cytotoxicity

Rubén M. Buey, **J. Fernando Díaz**, **José M. Andreu**, **Aurora O'Brate**, **Paraskevi Giannakakou**, **K. C. Nicolaou**, **Pradip K. Sasmal**, **Andreas Ritzén**, **and Kenji Namoto**

Mechanisms of Epothilone-Induced Microtubule Assembly

Microtubule assembly in the absence of ligands is a noncovalent nucleated condensation polymerization characterized by a cooperative behavior and the presence of a critical concentration, Cr, below which no significant formation of large polymers take place [32]. It can be demonstrated [45] that the apparent equilibrium constant for the growth reaction, i.e., the addition of a protomer to the polymer, is in good approximation, equal to the reciprocal critical concentration, $Kp = Cr^{-1}$, which renders the apparent standard free energy change of assembly amenable to simple measurement. Ligand-induced assembly is a more complex reaction in which an apparent critical concentration which holds on the ligand concentration is observed [32]. Ligand-induced tubulin assembly may proceed in two different pathways [32]: the ligand-facilitated pathway (elongation precedes binding, Equation S1) i.e., the binding of a tubulin dimer creates a new high affinity binding site for the ligand,

$$Tub + Mtb \overset{k_{el1}}{\rightleftharpoons} Tub-Mtb + Lig \overset{k_{bin1}}{\rightleftharpoons} Tub-Mtb-Lig \qquad (S1)$$

and the both possible ligand-mediated pathways (binding precedes elongation), which are thermodynamically equivalent: a) the ligand bind to unassembled tubulin and the ligated dimer has a higher affinity for the microtubules, so decreasing the critical concentration (Eq. S2A), b) the binding of a ligand to the end of the microtubule increases the affinity for the bind of the next dimer (Eq. S2B).

$$Mtb + Lig \overset{k_{bin2}}{\rightleftharpoons} Mtb-Lig + Tub \overset{k_{el2}}{\rightleftharpoons} Tub-Mtb-Lig \qquad (S2B)$$

$$Tub + Lig \overset{k_{bin2}}{\rightleftharpoons} Tub-Lig + Mtb \overset{k_{el2}}{\rightleftharpoons} Tub-Mtb-Lig \qquad (S2A)$$

By solving the mass law equations resulting from the reaction schemes, it can be calculated how the apparent elongation binding constant depends on the individual elongation and binding constants for both mechanisms.

If the reaction proceeds via the ligand-facilitated pathway the apparent elongation constant (the inverse of the dimer concentration in the supernatant) should linearly depend on the free concentration of ligand (Equation S3).

$$Kel_{app} = Kel1 \cdot (1 + [Ligand] \cdot Kb1) \qquad (S3)$$

Given two different ligands, at the same concentration, their assembly induction power should be linearly dependent on the binding constant of the ligand, independently of the specific effect that the ligand cause on tubulin.

If the reaction proceeds via the ligand-mediated pathways the apparent critical concentration should saturate with the ligand concentration (equation S4).

$$Kel_{app} = \frac{Kel2 \cdot Kbin2 \cdot [Ligand]}{(1 + Kbin2 \cdot [Ligand])} \qquad (S4)$$

So the measured critical concentration will depend on the elongation constant of the ligated dimer, which will depend on the specific effect that the ligand employed causes upon binding to a tubulin molecule.

It is possible as well that both mechanisms work; in this case the apparent critical concentration will saturate following equation (S5):

$$Kel_{app} = Kel2 \cdot Kbin2 \frac{[Ligand] + \frac{1}{Kbin1}}{(1 + Kbin2 \cdot [Ligand])} \qquad (S5)$$

In practice, since the ligand concentrations necessary to induce assembly free ligand are of the order of 10^{-6} M and $1/K_{bin1}$ is of the order of 10^{-7} to 10^{-9} M, the term $1/K_{bin1}$ can be neglected and so equation S5 becomes equivalent to eq.S4.

Epothilone- and paclitaxel-induced assembly saturate with ligand concentration (Figure 2 of this work and Figure 5 ref. 38) as it would be if it followed Equation S4, so its behavior is not what is suggested from Eq. S3. Although the linkage between ligand binding and ligand-induced assembly precludes the study at low ligand concentration, critical concentrations in the presence of overstoichiometric amounts of epothilone A calculated from the data of Figure 2 and plotted in the Figure S1 (solid circles) follow a saturating behavior as expected. It might be argued that a small fraction of inactive tubulin will deviate the linear behavior predicted from equation S3. Nevertheless since the critical concentrations of the more powerful epothilone analogs are much lower than these of epothilone A and B, the saturating behavior observed should not be due to this small fraction. In order to confirm so control experiments were performed in buffers with lower magnesium concentrations in which tubulin in supernatant is a higher percentage of the total tubulin, the same saturating behavior was observed. This behavior indicates that, a) the ligand-mediated pathways are involved in the epothilone induced assembly and b) the ligand-facilitated pathway is thermodynamically irrelevant since it does not contribute to the total free energy change of the assembly reaction and so it can be neglected. Moreover a ligand-facilitated pathway will result as predicted by equation S3 in an assembly induction power directly proportional to the binding constant, which is not the case since several compounds significantly deviate from the best regression line (Figure 4A). Following equation S5, it can be deduced that the measured Cr in saturation conditions (the experimental conditions) corresponds to the Cr of the ligated tubulin (or Cr of unligated tubulin to the ligated microtubule end) i.e., $1/K_{el2}$.

Moreover, the ligand-facilitated pathway can be also kinetically discarded. Since in the conditions of the study the reaction does not proceed in the absence of ligand, k_{el1} should be much lower than $k_{el2,}$ and at the ligand concentrations of the study, the concentration of unligated microtubules [Mtb] is negligible, the product k_{el1}*[Mtb] that following Equation S1 is the apparent kinetic rate of the ligand-facilitated pathway should be much lower than the product k_{el2}*[Mtb-Lig] which is the apparent kinetic rate of the ligand-mediated pathway.

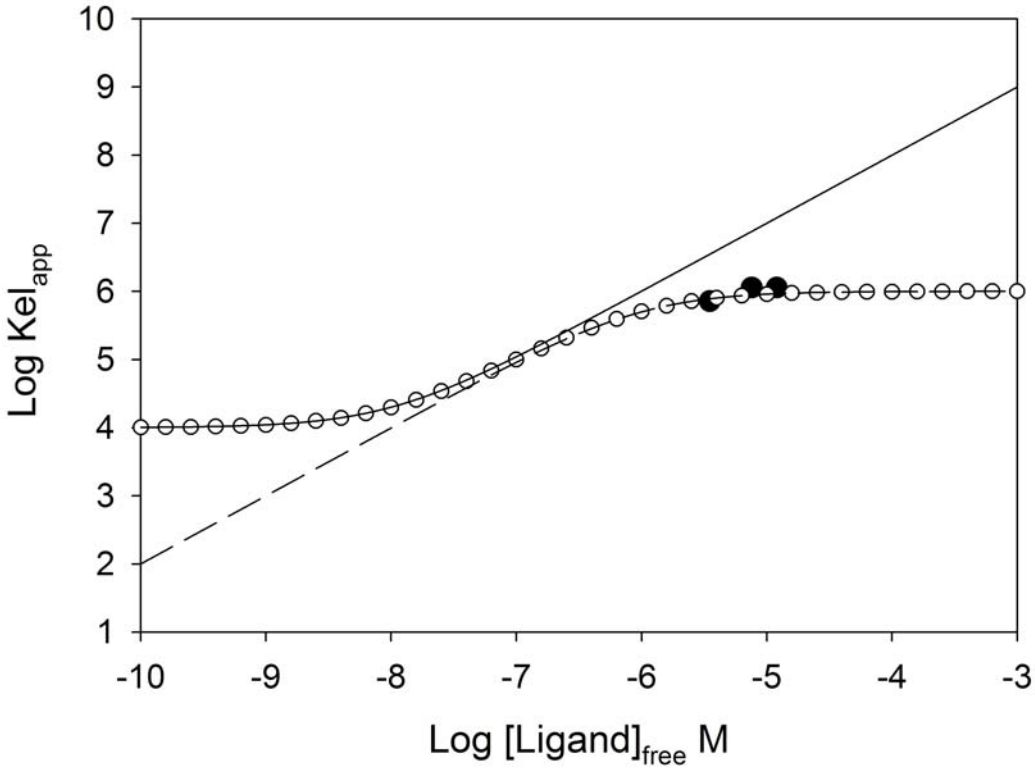

Figure S1.

Dependence of the apparent critical concentration of ligand-induced assembly on the ligand free concentration; with assembly following: (solid line) ligand-facilitated pathway, (dashed line) ligand-mediated pathway, (void circles line) both mechanisms work. Employed elongation and binding constants were the following: elongation constant of unligated tubulin K_{el1} 10^4 M^{-1}, binding constant of the ligand to assembled microtubules K_{bin1} 10^8 M^{-1}, binding constant of the ligand to unligated tubulin K_{bin2} 10^6 M^{-1}, elongation constant of ligated tubulin K_{el2} 10^6 M^{-1}. The solid circles are the apparent critical concentrations of GTP-tubulin in PEDTA7 GTP incubated with different overstoichiometric amounts of epothilone A. Data are from the experiment of Figure 2, free ligand concentrations were determined by HPLC as described in experimental procedures.